

# Accurate calculations of the WIMP halo around the Sun and prospects for its gamma ray detection

Sofia Sivertsson\*

*Department of Theoretical Physics, Royal Institute of Technology (KTH),  
AlbaNova University Center, 106 91 Stockholm, Sweden and  
The Oskar Klein Centre for Cosmoparticle Physics, Department of Physics,  
Stockholm University, AlbaNova University Center, 106 91 Stockholm, Sweden*

Joakim Edsjö†

*The Oskar Klein Centre for Cosmoparticle Physics, Department of Physics,  
Stockholm University, AlbaNova University Center, 106 91 Stockholm, Sweden  
(Dated: February 7, 2020)*

Weakly interacting massive particles (WIMPs) can be captured by heavenly objects, like the Sun. Under the process of being captured by the Sun, they will build up a population of WIMPs around it, which will eventually sink to the core. It has been suggested that this halo of WIMPs around the Sun could be a gamma ray source, possibly distinct enough to have nice detectable signature for WIMP dark matter. We here revisit this problem using detailed Monte Carlo simulations and detailed composition and structure information about the Sun to estimate the size of the gamma ray flux. Compared to earlier simpler estimates, we find that the gamma ray flux from WIMP annihilations in the Sun halo would be negligible; no current or planned detectors would be able to detect this flux.

## I. INTRODUCTION

The observational evidence for the need of dark matter is overwhelming (see e.g. [1]), but in spite of that, direct evidence for dark matter particles has not yet been found. One of the favourite classes of dark matter models, are Weakly Interacting Massive Particles (WIMPs), i.e. heavy particles with weak interaction strengths, as they would naturally be produced in right abundances during freeze-out in the early Universe (see e.g. [2]). There are many ways to search for WIMPs, e.g. via direct detection, or via indirect detections, like neutrinos from the Sun/Earth, gamma rays from annihilations in the galactic halo or charged cosmic rays from annihilations in the galactic halo. We will here focus on another idea, proposed by Strausz [3] in 1999. The idea is that while WIMPs are being captured by the Sun, they will move on bound orbits outside the Sun, making up a halo of WIMPs around it. Pair-wise annihilations of WIMPs in this halo could occur and (if the density would be high enough), produce a detectable flux of e.g. gamma rays. This type of gamma ray flux has been searched for by e.g. the Milagro [4] detector.

Strausz came to the conclusion that this gamma ray signal would be measurable or that if no such signal is seen, one would be able to constrain parameters in the WIMP model. However, Strausz' calculation imposes many approximations and in a later preprint by Hooper [5], it was found that the flux of gamma rays is much smaller than Strausz' estimates and a detection of this gamma ray signal would require unrealistically large telescope areas. In both these calculations many simplifying approximations are made; for example radial orbits are assumed, the WIMPs real orbits are not followed with realistic solar models. Another calculation was performed by Fleysher [6], that got even higher gamma ray fluxes than in Strausz' calculation.

To clarify the discrepancies between these earlier estimates, we have here performed a much more thorough calculation of the WIMP density around the Sun via detailed Monte Carlo simulations. We let WIMPs from the galactic halo scatter in the Sun and follow the WIMPs on their orbits (taking full account of the non-Keplerian nature of the orbits inside the Sun), letting them interact over and over again until they are fully inside the Sun. For each WIMP we simulate, we can calculate how much it contributes to the WIMP halo density around the Sun and by summing up the contributions from the entire WIMP population, we can estimate the WIMP halo density around the Sun. We finally calculate the gamma ray signal from WIMP annihilations in this halo, which can be compared with the Milagro searches for a gamma ray signal of this kind [4]. We will also calculate predicted fluxes for future gamma ray detectors and compare with expected backgrounds.

---

\*Electronic address: sofiasi@kth.se

†Electronic address: edsjo@physto.se

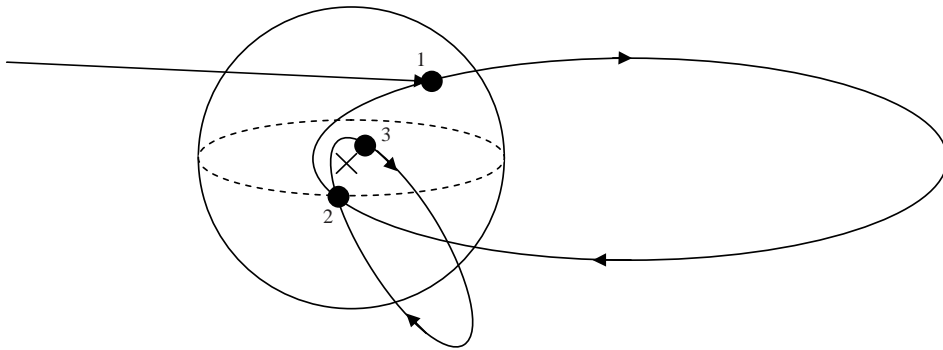


FIG. 1: An example of a WIMP being captured by the Sun. A WIMP from the Milky Way halo population scatters at point 1 as it passes through the Sun. If enough energy is lost the WIMP ends up on a bound orbit which it travels in, typically many laps, until it scatters again in point 2 to an orbit with lower energy. In this example the WIMP has, after the scatter in point 3, lost enough energy to end up in an orbit completely hidden inside the Sun and is no longer of any interest to us. Note that in the figure the orbits are entirely elliptical, whereas in reality (and in our simulations), they are slightly non-elliptical inside the Sun.

## II. THE WIMP CAPTURE PROCESS

As WIMPs from the Milky Way halo pass through the Sun, some of them will scatter off nucleons in the Sun and lose energy. If enough energy is lost in the scatter, the WIMP becomes unable to escape the Sun's gravitational well and ends up in some orbit around the centre of the Sun. The bound WIMP will eventually scatter again in the Sun and as this energy loss continues the WIMP will at some stage end up in an orbit which is completely hidden inside the Sun. The WIMP capture process is illustrated in figure 1.

Due to the smallness of the scatter cross section, a bound WIMP typically survives many passages in the Sun before it scatters again. Also, WIMPs which scatter in the outskirts of the Sun can end up on orbits only passing through the less dense outer regions of the Sun, making the orbits very long lived.

Especially for scatters off lighter elements, the WIMPs are much heavier than the nuclei they scatter off, making them typically lose only small fractions of their energies in each scatter. This implies that a WIMP often have to scatter a number of times before being absorbed completely by the Sun. Also, the first orbits of a captured WIMP can easily reach very far from the Sun.

To get good accuracy of our predictions, we follow the WIMPs through the Sun on their actual orbits and taking the actual solar environment (as a function of radius), and details of the scattering process into account.

All these intermediate orbits contribute to the WIMP density around the Sun, building up a WIMP halo. WIMP annihilations within this halo give rise to high energy gamma rays, where the only background is cosmic ray interactions with the solar chromosphere [7] and up-scattering of solar photons via inverse Compton scattering from cosmic ray electrons [8, 9, 10]. Also, the Sun is opaque to gamma rays and hence shields against the diffuse gamma ray background.

## III. BUILD-UP OF THE WIMP HALO

### A. The WIMPs' first scatter in the Sun

Following the notation of Gould [11], the total number of WIMPs that scatter in a shell of a given radius in the Sun per unit time and velocity is given by

$$4\pi r^2 dr \frac{\sigma \rho(r)}{m} w^2 \frac{f(u)}{u} du, \quad (1)$$

where  $f(u)$  is the velocity distribution of the WIMPs in the Milky Way halo, in the Sun's reference system and infinitely far away,  $m$  is the mass of the nucleus in the Sun which the WIMP scatters off,  $\sigma$  is the scatter cross section on that nucleus,  $u$  is the WIMP velocity at infinity,  $v$  is the escape velocity at the shell,  $w$  is the velocity of the WIMP in the shell,  $r$  is the radius of the shell and  $\rho(r)$  is the density of element  $m$  at radius  $r$ . We will later denote the WIMP mass with  $M$ . The expression above should eventually be summed over the elemental abundances in the Sun. We use the solar model of [12] with heavy element abundances from [13] as implemented in DarkSUSY [14]. In total we include the 16 most important elements in the Sun in our calculation.

Assuming the velocities of the WIMPs in the Milky Way halo to be Maxwell-Boltzmann distributed, the velocity distribution in the Sun's reference frame is [11]

$$\frac{f(u)}{u} du = n_W \sqrt{\frac{6}{\pi}} \frac{1}{v_\odot \bar{v}} \exp\left(-\frac{3v_\odot^2}{2\bar{v}^2}\right) \exp\left(-\frac{3u^2}{2\bar{v}^2}\right) \sinh\left(\frac{3uv_\odot}{\bar{v}^2}\right) du, \quad (2)$$

where  $v_\odot$  is the Sun's velocity orbiting the Milky Way centre and  $\bar{v}$  is the WIMP velocity dispersion in the halo, here taken to be  $\bar{v} = 270$  km/s.  $n_W = \rho_W/M$  is the number density of WIMPs in our region of the Milky Way halo, where we take  $\rho_W = 0.3$  GeV cm<sup>-3</sup>.

For further use the WIMPs' energy distribution will be more useful than the velocity distribution; expression (2) can be rewritten as

$$\frac{f_{\mathcal{E}}(\mathcal{E})}{\mathcal{E}} d\mathcal{E} = n_W \sqrt{\frac{3}{\pi}} \frac{1}{v_\odot \bar{v}} \exp\left(-\frac{3v_\odot^2}{2\bar{v}^2}\right) \exp\left(-\frac{3\mathcal{E}}{\bar{v}^2}\right) \sinh\left(\frac{3v_\odot}{\bar{v}^2} \sqrt{2\mathcal{E}}\right) \frac{1}{\sqrt{\mathcal{E}}} d\mathcal{E}, \quad (3)$$

where  $\mathcal{E}$  is the reduced energy, defined as the WIMP's energy (kinetic plus potential) divided by the WIMP mass, i.e. for a captured WIMP  $\mathcal{E} < 0$ . Furthermore  $\mathcal{E}_k$  is the reduced kinetic energy and  $\mathcal{E}_p$  is the reduced potential energy at some radius.

Rewriting expression (1) now yields the number of WIMPs which scatter in a shell in the Sun per unit time and reduced energy<sup>1</sup>

$$\frac{d^2\Gamma}{d\mathcal{E} dr} = 8\pi r^2 \frac{\sigma\rho(r)}{m} (\mathcal{E} - \mathcal{E}_p) \frac{f_{\mathcal{E}}(\mathcal{E})}{\mathcal{E}} \quad (4)$$

expressed using the reduced energy the WIMP has before it scatters.

### 1. The WIMPs' energy distribution after their first scatter

When a WIMP interacts with a nucleus it scatters from the reduced kinetic energy before the scatter,  $\mathcal{E}_k$ , to the reduced kinetic energy after the scatter,  $\tilde{\mathcal{E}}_k$ , which, as for general elastic scatter, fulfils the relation

$$\left(\frac{M-m}{M+m}\right)^2 \mathcal{E}_k \leq \tilde{\mathcal{E}}_k \leq \mathcal{E}_k \quad (5)$$

with all  $\tilde{\mathcal{E}}_k$  in this interval being equally probable. Note that it is the energy loss and not the loss in velocity that is uniformly distributed.

This means that a WIMP with the reduced energy  $\tilde{\mathcal{E}}_k$  can only have scattered from reduced energies fulfilling

$$\tilde{\mathcal{E}}_k \leq \mathcal{E}_k \leq \left(\frac{M+m}{M-m}\right)^2 \tilde{\mathcal{E}}_k, \quad (6)$$

which written in terms of total reduced energy  $\mathcal{E} = \mathcal{E}_k + \mathcal{E}_p$  becomes

$$\tilde{\mathcal{E}} \leq \mathcal{E} \leq \left(\frac{M+m}{M-m}\right)^2 \tilde{\mathcal{E}} - \frac{4Mm}{(M-m)^2} \mathcal{E}_p. \quad (7)$$

Note that  $\mathcal{E} \geq 0$  since the particles in the Milky Way halo are not bound to the Sun, while the sign of the reduced energy after the scatter,  $\tilde{\mathcal{E}}$ , is not determined.

---

<sup>1</sup> Note that

$$\lim_{u \rightarrow 0} \frac{f(u)}{u} = 0 \quad \text{but} \quad \lim_{\mathcal{E} \rightarrow 0} \frac{f_{\mathcal{E}}(\mathcal{E})}{\mathcal{E}} \neq 0$$

and hence the number of scatters per unit time and velocity vanishes as  $u \rightarrow 0$  while the number of scatters per unit time end energy does not vanish as  $\mathcal{E} \rightarrow 0$ .

The number of WIMPs which scatter to a certain reduced energy,  $\tilde{\mathcal{E}}$ , in a given shell in the Sun, per unit time is then

$$\frac{d^2\Gamma}{d\tilde{\mathcal{E}} dr} = 2\pi r^2 \frac{\rho(r)}{m} \frac{(m+M)^2}{Mm} \int_{\tilde{\mathcal{E}}}^{u.l.} \sigma \frac{f_{\mathcal{E}}(\mathcal{E})}{\mathcal{E}} \theta(\mathcal{E}) d\mathcal{E}, \quad (8)$$

where  $u.l. = \left(\frac{M+m}{M-m}\right)^2 \tilde{\mathcal{E}} - \frac{4Mm}{(M-m)^2} \mathcal{E}_p$

which is the integral of (4) with integration limits given by (7). Here  $\theta$  is the Heaviside function, which is required since  $\tilde{\mathcal{E}}$  can be negative while  $\mathcal{E}$  is always positive.

The above expression has been normalised by multiplying by the reciprocal of the interval length in (5)

$$\frac{1}{\mathcal{E}_k} \frac{(M+m)^2}{4Mm}. \quad (9)$$

## 2. Form factor suppression of the scattering cross section

For scatter off nuclei larger than the proton the cross section depends on the energy loss in the scatter. For scatters with low momentum transfer the wave functions of the different nucleons in the nuclei may be viewed as coherent, making the cross section increase as the square of the number of nucleons in the nucleus,  $A^2$ . For higher momentum transfer this coherence breaks down. This suppression is taken into account by introducing an exponential form factor, suppressing high energy transfers, i.e. high  $\Delta\mathcal{E}$  [11]

$$\exp\left(-\frac{\Delta\mathcal{E}}{\mathcal{E}_0}\right) \quad (10)$$

with

$$\mathcal{E}_0 \equiv \frac{3\hbar^2}{2mMR^2} \quad \text{and} \quad R \sim \left[0.91 \left(\frac{m}{GeV}\right)^{1/3} + 0.3\right] \cdot 10^{-15} \text{ m}, \quad (11)$$

where  $R$  is an estimate of the radius of the nucleus [15].

Introducing a form factor, expression (8) can be written as

$$\frac{d^2\Gamma}{d\tilde{\mathcal{E}} dr} = 2\pi r^2 \frac{\rho(r)}{m} \tilde{\sigma} \frac{(m+M)^2}{Mm} \int_{\tilde{\mathcal{E}}}^{u.l.} \frac{f_{\mathcal{E}}(\mathcal{E})}{\mathcal{E}} \exp\left(\frac{\tilde{\mathcal{E}} - \mathcal{E}}{\mathcal{E}_0}\right) \theta(\mathcal{E}) d\mathcal{E}, \quad (12)$$

where  $u.l. = \left(\frac{M+m}{M-m}\right)^2 \tilde{\mathcal{E}} - \frac{4Mm}{(M-m)^2} \mathcal{E}_p$

where  $\tilde{\sigma}$  refers to the total low-energy cross section (i.e. without the form factor suppression). Since the Sun contains many different elements,  $\rho(r)$  in (12) should be viewed as the density of a specific element and then summed over all relevant elements in the Sun, with the form factor removed for hydrogen.

Expression (12) describes the distribution of WIMPs after their first scatter in the Sun, illustrated in figure 2. Hydrogen is the only significant element in the Sun which couples axially to the WIMP so if spin dependent scatter,  $\sigma_{SD}$ , dominates the WIMPs will scatter effectively only off hydrogen. If spin independent scatter,  $\sigma_{SI}$ , dominates scatter off hydrogen is insignificant while helium is not. Even though the abundance of heavier elements in the Sun is small, they can still play an important role due to the increase of phase space accessible in the scatter. Since the WIMPs scatter off nuclei of different masses in the two scenarios the dynamics is quite different. Note that both  $\sigma_{SD}$  and  $\sigma_{SI}$  refer to the scattering cross sections off protons (as these are the quantities usually used to quantify the size of the scattering cross sections). We will use optimistic values of  $\sigma_{SI} = 10^{-5}$  pb and  $\sigma_{SD} = 10^{-3}$  pb, but as well will see in section IV A, our results do not depend on the values chosen for the cross sections (within reasonable limits).

In the upper graph in figure 2 the WIMPs scatter only off hydrogen which makes the energy loss in the scatter quite small, making the Sun only capable of capturing the low energy tail of the Milky Way WIMP population. This is seen in the graph in that the majority of the WIMPs scatter to an energy greater than zero. On the other hand the WIMPs have to scatter many times before being buried inside the Sun, allowing greater contributions to the WIMP density outside the Sun.

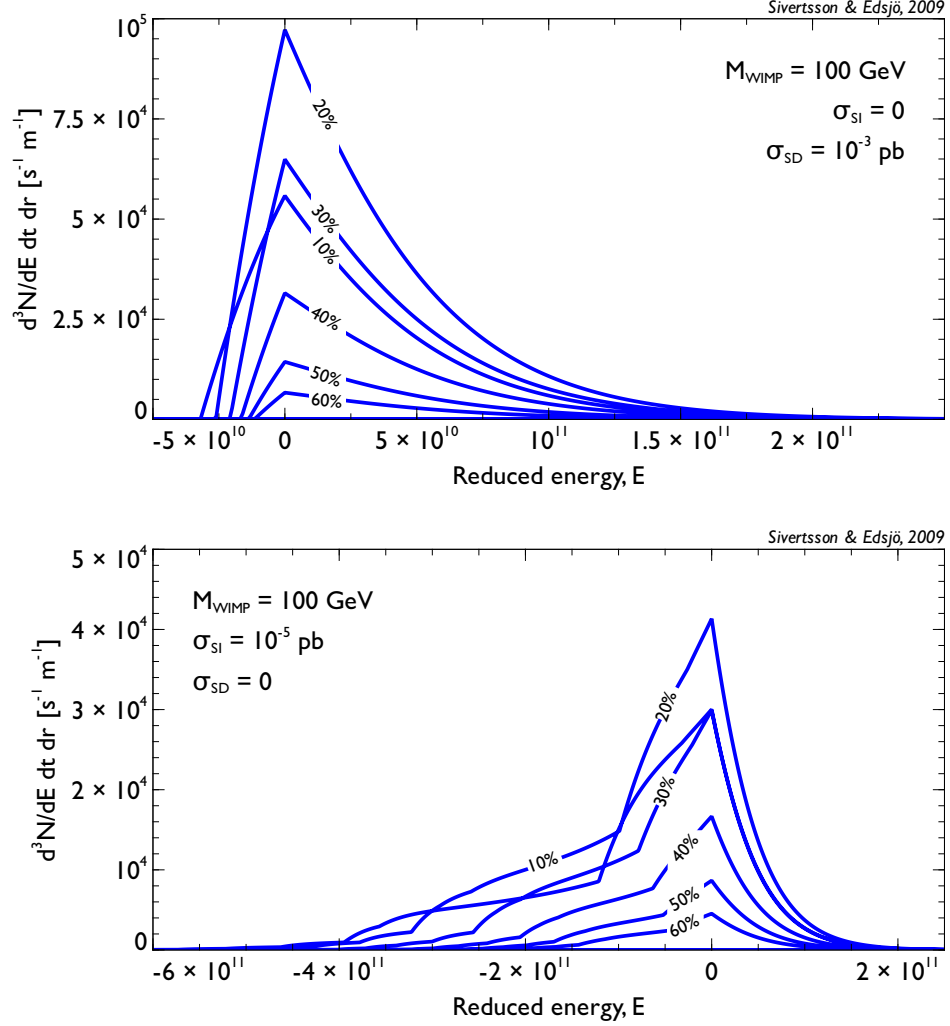


FIG. 2: Plot of expression (12) for spin dependent scatter,  $\sigma_{SD} = 10^{-3}$  pb, and spin independent scatter,  $\sigma_{SI} = 10^{-5}$  pb, respectively being dominant. The graphs show the distribution of scattered WIMPs after their first scatter in the Sun, expressed as the number of scattered WIMPs per unit time, unit reduced energy after the scatter and unit radius in the Sun. The different lines correspond to different radii in the Sun where the WIMPs scatter, showing the shells with radius 10%, 20%, ..., 60% of the Sun's radius, the graphs hence illustrates surfaces. The smaller the radius of the illustrated shell, the further to the left the graph has non-zero values, i.e. the smaller the possible reduced energy is after the scatter. The WIMP mass is here set to 100 GeV.

In the lower graph in figure 2 the spin-independent scatter dominate making the WIMPs scatter mostly off heavier nuclei and hence, on average, lose a lot more energy in the scatter. This makes the WIMPs much more likely to be captured in the Sun's potential well but as seen in the graph some will immediately disappear inside the Sun since a WIMP needs a reduced energy of at least  $\mathcal{E} = -\frac{GM_{\odot}}{R_{\odot}} = -1.9 \cdot 10^{11} \text{ m}^2/\text{s}^2$  to be energetic enough to reach the region outside of the Sun.

The pointyness of the graphs in figure 2 comes from the discontinuity of the integrand which is related to the footnote associated to eq. (4). The function  $\frac{f_{\mathcal{E}}(\mathcal{E})}{\mathcal{E}}\theta(\mathcal{E})$  jumps from zero to its maximum value at  $\mathcal{E} = 0$ .

WIMPs which scatter close to the centre of the Sun have higher velocities in the scatter and hence normally lose a larger fraction of their total energy in the scatter. This is the reason for inner shell curves in figure 2 being non-zero for lower values of  $\tilde{\mathcal{E}}$ .

Integrating expression (12) over  $r$  and  $\tilde{\mathcal{E}}$ , for  $\tilde{\mathcal{E}} < 0$ , gives the total capture rate of WIMPs by the Sun. The total capture rate is of interest in computing the neutrino flux from annihilating WIMPs in the centre of the Sun. This can also be calculated using the DarkSusy program [14] and is in excellent agreement with our results.

### 3. The scatter angle after the WIMPs' first scatter

To determine the orbit of the captured WIMP one, besides the energy distribution and the place of scatter, also needs the scatter angle,  $\alpha$ , defined as the angle between the path of the scattered WIMP and the radial direction from the centre of the Sun.

In this work spherical symmetry is assumed, i.e. taking all possible directions for a specific first scatter to be equally probable. The small scatter probability for a WIMP passing through the Sun makes it equally likely for the WIMP to scatter on its way out as on its way in to the Sun. The Sun's velocity and gravitational influence could give rise to some anisotropy. This would, however, be somewhat smoothened as the WIMP capture process continues.

All scatter directions being equally probable after the first scatter gives the probability distribution for  $\alpha$

$$\frac{2\pi \sin(\alpha)d\alpha}{4\pi} = \frac{1}{2} \sin(\alpha)d\alpha, \quad \text{where } 0 \leq \alpha \leq \pi. \quad (13)$$

### B. The orbits and lifetimes of the captured WIMPs

The reduced energy,  $\mathcal{E}$ , and reduced angular momentum,  $\mathcal{J}$ , of a captured WIMP are given by

$$\mathcal{E} = \frac{v^2}{2} + \mathcal{E}_p(r), \quad (14)$$

$$\mathcal{J} = rv|\sin \alpha| = r\sqrt{2(\mathcal{E} - \mathcal{E}_p(r))}|\sin \alpha|, \quad (15)$$

where  $r$  is the radius where the scatter took place and  $v$  the velocity the WIMP scattered to. The reduced potential energy at the scatter,  $\mathcal{E}_p$ , is given by a numerical function for the gravitational potential inside the Sun.

The energy and angular momentum together fully specify the orbit, up to the spherical symmetry. It will be useful for us to find the minimal and maximal distances of the orbit to the centre of the Sun,  $r_{\min}$  and  $r_{\max}$ . These two points are the only points in the orbit fulfilling  $\mathcal{J} = r\sqrt{2(\mathcal{E} - \mathcal{E}_p(r))}$ . We are here only interested in WIMPs which spend time both inside and outside the Sun, i.e. WIMPs on orbits fulfilling  $r_{\min} < R_{\odot} < r_{\max}$ . As the WIMPs were captured by scatters in the Sun their future orbits will always be partly inside the Sun unless disturbed in some way, e.g. by the planets; this is not taken into account in these calculations. Outside the Sun the gravitational potential is simply  $\mathcal{E}_p = -GM_{\odot}/r$ , allowing us to simply solve for  $r_{\max}$

$$r_{\max} = -\frac{GM_{\odot}}{2\mathcal{E}} + \sqrt{\left(\frac{GM_{\odot}}{2\mathcal{E}}\right)^2 + \frac{\mathcal{J}^2}{2\mathcal{E}}}. \quad (16)$$

Inside the Sun the gravitational potential is not so simple and hence  $r_{\min}$  can not be found in such a simple way as  $r_{\max}$ . The orbit everywhere fulfils  $\mathcal{J}^2 \leq (rv)^2 = 2r^2(\mathcal{E} - \mathcal{E}_p(r))$  with equality only for  $r$  equal to  $r_{\min}$  or  $r_{\max}$ . For the evaluation of the rather unnatural points inside the orbit,  $r < r_{\min}$ , one can show that  $\mathcal{J}^2 > 2r^2(\mathcal{E} - \mathcal{E}_p(r))$ . It is then easy to determine  $r_{\min}$  from a numerical binary search.

#### 1. The density contribution to the WIMP halo before the WIMP scatters again.

To find the density of WIMPs around the Sun one needs to know what fraction of its time an orbiting WIMP spends at different distances from the Sun. We will later look closer at the radial velocities, and from eq. (22) one finds

$$dt = \frac{r}{\sqrt{2(GM_{\odot} + \mathcal{E}r)r - \mathcal{J}^2}}|dr|. \quad (17)$$

This expression diverges for  $r = r_{\min}$  and  $r = r_{\max}$  but the integral converges everywhere. Since the velocity is lower in the outer regions of the orbit the WIMP also spends most of its time there.

Integrating the right hand side of expression (17), using *Mathematica*, gives the primitive function

$$-2\frac{GM_{\odot}}{(-2\mathcal{E})^{3/2}} \arctan\left(\frac{2\mathcal{E}r + GM_{\odot}}{\sqrt{-2\mathcal{E}}\sqrt{2r(GM_{\odot} + \mathcal{E}r) - \mathcal{J}^2}}\right) + \frac{1}{\mathcal{E}}\sqrt{2r(GM_{\odot} + \mathcal{E}r) - \mathcal{J}^2}, \quad (18)$$

which is used to obtain the time the WIMP spends in a certain radial interval. A factor of 2 has also been added to the integral since an orbiting WIMP passes some radius twice or not at all.

For the orbits investigated here the WIMP typically spends most of its time outside the Sun. The total time,  $T$ , it takes for the WIMP to complete a full lap in an elliptical orbit is

$$T = \frac{\pi}{\sqrt{2}} \frac{GM_{\odot}}{(-\mathcal{E})^{3/2}}. \quad (19)$$

The density contribution also depends on how many passages the WIMP survives before it scatters again. On average, the density contribution of the WIMP's first lap in the orbit is higher than the density contribution of the second lap, since there is some probability for the WIMP to scatter again before commencing its second lap. The probability for the WIMP to scatter twice in one solar passage is immensely small and can be neglected.

The probability for the bound WIMP to survive  $n$  laps without scattering in the Sun is  $q^n = (1 - P)^n$  with  $P$  being the probability for the WIMP to scatter in one passage.

The total density contribution by a WIMP in a given orbit, integrated over time, is, on average

$$\rho_0(1 + q + q^2 + \dots + q^n) = \rho_0 \frac{1 - q^{n+1}}{1 - q} = \rho_0 \frac{1 - (1 - P)^{n+1}}{P}, \quad (20)$$

where  $\rho_0$  is the density contribution from the first lap in the orbit. The finite age, of approx 4.5 billion years, of the Sun gives a cut in the sum since no orbits can be older than this. The maximum number of laps a WIMP can have fulfilled in a given orbit is  $n = (4.5 \cdot 10^9 \text{ yr})/T$ , with  $T$  being the orbit time, as in expression (19).

In practice, the finite age of the Sun is important only for very low scatter cross sections. Then also the orbits which these long lived WIMPs scatter to should be removed. In our runs with very low cross section, we have taken this into account.

## 2. The scatter probability for a bound WIMP passing through the Sun

The probability for collision when a WIMP passes a shell in the Sun is given by

$$\sigma \frac{\rho(r)}{m} v \cdot 2 \frac{dr}{|v_r|}, \quad (21)$$

where  $\rho$  and  $m$  refer to the density and mass, respectively, of the target nucleus. The above expression is then summed over the relevant elements. Also, the scatter cross section can depend on the energy loss in the scatter, which depends on the WIMP velocity and hence the radius of the scatter. The above expression comes from the number of scatters per unit time ( $\sigma n v$ ) times the time the WIMP spends in a given shell taken twice, since the particle intersects a shell twice or not at all during one lap.

From  $v$  and  $\mathcal{J}$  for a particle one easily determines the radial velocity component

$$\frac{v}{|v_r|} = \frac{rv}{\sqrt{r^2 v^2 - \mathcal{J}^2}}. \quad (22)$$

Hence, the probability for the WIMP to scatter in the Sun during one lap is

$$P = \frac{2}{m} \int_{r_{\min}}^{R_{\odot}} \sigma \rho(r) \frac{rv}{\sqrt{r^2 v^2 - \mathcal{J}^2}} dr, \quad (23)$$

where  $v^2 = 2\mathcal{E} - 2\mathcal{E}_p(r)$  and  $r_{\min}$  is easily determined numerically, as previously discussed. If the WIMP scatters off hydrogen, the cross section does not depend on the energy loss and it is straightforward to evaluate eq. (23).

Accounting for the form factor suppression of the cross section needs some further treatment. For a bound WIMP passing the Sun once in an orbit with reduced energy,  $\mathcal{E}$ , and reduced angular momentum,  $\mathcal{J}$ , the probability to scatter off a given element in a (possible) shell in the Sun, given by the radius  $r$ , to a certain, possible energy  $\tilde{\mathcal{E}}$  is given by

$$\frac{1}{\mathcal{E}_k} \frac{(M + m)^2}{4Mm} e^{-\Delta\mathcal{E}/\mathcal{E}_0} \tilde{\sigma} \frac{\rho(r)}{m} 2 \frac{dr}{v_r} d\tilde{\mathcal{E}}, \quad (24)$$

where the rightmost part is simply expression (21). The first part of expression (24) is the factor given in expression (9) times the form factor suppression.

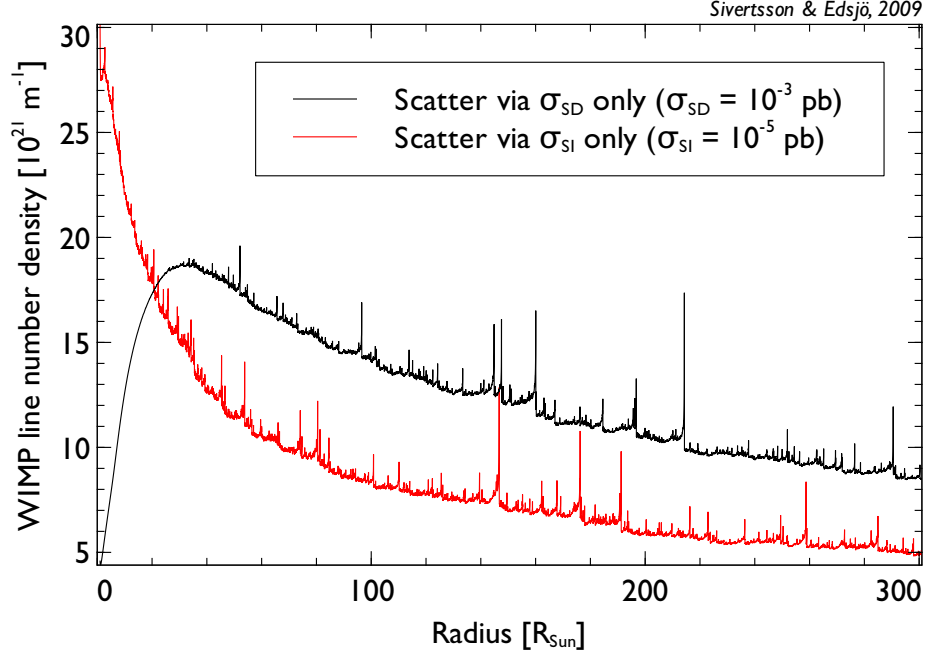


FIG. 3: The line density around the Sun of WIMPs that have scattered exactly once in the Sun. The black curve is for spin dependent scatters dominating, using  $\sigma_{SD} = 10^{-3}$  pb,  $\sigma_{SI} = 0$  and is generated by a calculation of 1 million scattered WIMPs. The red curve is for spin independent scatters dominating, using  $\sigma_{SI} = 10^{-5}$  pb,  $\sigma_{SD} = 0$  and is the result of 100 000 simulated scattered WIMPs. For both curves the WIMP mass is  $M = 100$  GeV. The Earth is approximately 215 solar radii away from the Sun.

The probability for the WIMP to scatter to any possible energy in a given shell during one lap in the orbit is given by the integral of expression (24) over the possible values of  $\tilde{\mathcal{E}}$  and then summed over the different elements in the Sun

$$\frac{v}{v_r} \frac{1}{\mathcal{E}_k} \left( 2\sigma_{SD} \frac{\rho(r)}{m} + \sum_2^{16} \frac{(M+m)^2}{2Mm} \tilde{\sigma}_{SI} \frac{\rho(r)}{m} \mathcal{E}_0 \left[ 1 - \exp \left( -\frac{4Mm}{(M+m)^2} \frac{\mathcal{E}_k}{\mathcal{E}_0} \right) \right] \right), \quad (25)$$

where  $v/v_r$  is given by expression (22). The density of the particular element,  $\rho(r)$ , and the mass,  $m$ , depend on the element summed over. The leftmost term refers to hydrogen, which is the only element here with spin dependent scatter cross section to the WIMP.  $\tilde{\sigma}_{SI}$  here refers to the total low-energy spin-independent cross section that is related to the usually used spin-independent cross section on a proton,  $\sigma_{SI}$ , via

$$\tilde{\sigma}_{SI} = \sigma_{SI} A^2 \left( \frac{Mm}{M+m} \right)^2 \left( \frac{Mm_p}{M+m_p} \right)^{-2} \quad (26)$$

where  $m_p$  is the mass of the proton and  $A$  is the atomic number of the target nucleus.

The probability for the captured WIMP to scatter during one lap in its orbit is then given by the integral of the above expression over the radii in the Sun that the WIMP passes through in its orbit.

### 3. The density contribution of the WIMPs which have only scattered once

The analysis is now sufficient to calculate the density around the Sun of WIMPs which have scattered exactly once in the Sun. This is done through making a Monte Carlo simulation, simulating a large number of captured WIMPs according to the energy distribution after their first scatter, given by expression (12). This is described in the first part of section III D, which describes the structure of the final full Monte Carlo. The resulting density contribution of the WIMPs which have scattered only once is shown in figure 3. This graph shows the line number density of WIMPs around the Sun, i.e. to get the number density we have to divide by  $4\pi r^2$ .



The unevenness in figure 3 is simply because the number of simulated WIMPs is finite. Some simulated orbits, only intersecting the outer region of the Sun, are quite stable and the density contribution for a given orbit diverges as  $r$  reaches  $r_{\max}$ , giving rise to the peaks in the graph.

WIMPs which scatter only off hydrogen cannot lose enough energy in one scatter to end up on orbits which are entirely close to the Sun; this is why the black curve in figure 3 is smooth for small radii, i.e. for  $r < \min(r_{\max})$ . The orbiting WIMPs spend most of their time in the outer regions which is why the same curve rises with radius for small radii.

Taking into account the fact that the orbits are not perfect ellipses inside the Sun is found to increase the calculated line number density by roughly 20%. This is because the true orbits do not come as far into the dense central regions in the Sun as purely elliptical orbits would, which increases the life time of the true orbits since the scatter probability decreases.

### C. Subsequent scatters in the Sun

In general a WIMP scatters many times before its orbit becomes completely hidden inside the Sun. Also these intermediate orbits contribute to the WIMP density, especially in the region close to the Sun.

The radius of the point of scatter and the type of nucleus involved can in the Monte Carlo be extracted from expression (25), since this is really the distribution of the scatter parameters for a given orbit. Knowing the place of scatter and the elements involved, the distribution of the energy loss in the scatter is found by expression (24).

To find the WIMP's angular momentum after the scatter,  $\tilde{J}$ , requires some further treatment. Once the properties of the new orbit are determined the contribution to the halo density can be calculated in the same way as for the WIMPs which have only scattered once.

Using conservation of energy and momentum in the scatter and the general relation  $p^2 = \mathbf{p} \cdot \mathbf{p} = 2ME_k$  one can derive the relation

$$\mathbf{p} \cdot \tilde{\mathbf{p}} = (M - m)E_k + (M + m)\tilde{E}_k, \quad (27)$$

where  $\mathbf{p}$  and  $\tilde{\mathbf{p}}$  are the momentum before and after the scatter, respectively. Dividing  $\tilde{\mathbf{p}}$  and  $\mathbf{r}$  in components parallel ( $\tilde{p}_{\parallel}$  and  $r_{\parallel}$ ) and orthogonal ( $\tilde{p}_{\perp}$  and  $r_{\perp}$ ) to  $\mathbf{p}$ , using (27) and  $\mathbf{p} \cdot \tilde{\mathbf{p}} = p\tilde{p}_{\parallel}$  gives

$$\tilde{p}_{\parallel} = \frac{(M - m)E_k + (M + m)\tilde{E}_k}{p} \quad \text{and} \quad \tilde{p}_{\perp}^2 = \tilde{p}^2 - \tilde{p}_{\parallel}^2. \quad (28)$$

Using  $J = |\mathbf{J}| = r_{\perp}p$  also  $r_{\perp}$  and  $r_{\parallel}$  are easily determined since both  $p$  and  $J$  are known.

The modulus of the angular momentum after the scatter can be evaluated as

$$|\tilde{\mathbf{J}}|^2 = \left| \begin{pmatrix} r_{\perp} \\ 0 \\ r_{\parallel} \end{pmatrix} \times \begin{pmatrix} \tilde{p}_{\perp} \cos \phi \\ \tilde{p}_{\perp} \sin \phi \\ \tilde{p}_{\parallel} \end{pmatrix} \right|^2 = r^2 \tilde{p}_{\perp}^2 \sin^2 \phi + (r_{\parallel} \tilde{p}_{\perp} \cos \phi - r_{\perp} \tilde{p}_{\parallel})^2. \quad (29)$$

The azimuthal angle  $\phi$  is arbitrary in any given scatter and is hence generated as a random number in the Monte Carlo simulation.

### D. Monte Carlo

The actual calculation of the density of the Sun's WIMP halo is implemented through constructing a Monte Carlo simulating the capture process of a large number of WIMPs. The Monte Carlo is constructed as follows.

1. The Monte Carlo starts from the distribution of WIMPs which have scattered once to bound orbits. This distribution of WIMP interaction points, energy after the scatter and scatter element (from the solar model) is given by eq. (12); this distribution is also shown in figure 2. Having picked a WIMP according to this distribution, the scatter angle is picked from eq. (13), giving the final piece of information required to calculate the WIMPs angular momentum.
2. The density contribution by the WIMP in the orbit, before it scatters again, is then calculated. The line density contribution in a radial interval for one lap in the orbit is given by eq. (18). This is then multiplied with the average number of laps that a WIMP in such an orbit survives, which is given by eq. (20) and eq. (23).

3. The shell in the Sun in which the WIMP scatters next time is picked, using the expression for the scatter probability in the passage of a shell, given by eq. (25). The type of element the WIMP scatters to in the shell is then chosen according to the elemental abundance in the Sun.
4. The WIMPs energy loss in the scatter and its new angular momentum is determined, as described in section III C.
5. If the WIMP's new orbit is still energetic enough to be partly outside the Sun, i.e. if  $r_{\max}$  in eq. (16) is greater than  $R_{\odot}$ , the simulation continues with step 2, continuing to add to the WIMP density around the Sun.
6. If the WIMP has lost enough energy to be completely hidden inside the Sun it is no longer relevant here. The simulation of a new scattered WIMP starts from step 1.
7. When the desired number of captured WIMPs are simulated the result is weighted with the capture rate, which is found by integrating eq. (12) over  $r$  and  $\tilde{\mathcal{E}}$  for  $\tilde{\mathcal{E}} < 0$ , to get the real density.

#### IV. THE WIMP NUMBER DENSITY IN THE HALO

The constructed Monte Carlo has, as described in the above section, simulated the capture process, giving the density of WIMPs around the Sun. The simulations have been made for different WIMP masses and for both spin dependent and spin independent cross section being dominant. In total we have simulated about  $10^7$  WIMPs from first scatter to complete solar entrapment. The results of these simulations are shown in figure 4. The line number density can be well approximated by

$$n^{SD} = 10^{25.21-1.015x} \left( \frac{r}{R_{\odot}} \right)^{-0.48} \text{ m}^{-1}, \quad (30)$$

$$n^{SI} = 10^{23.71-0.2332x-0.1056x^2} \left( \frac{r}{R_{\odot}} \right)^{-0.40} \text{ m}^{-1}, \quad (31)$$

$$\text{with } x = \log_{10} \left( \frac{M}{1 \text{ GeV}} \right). \quad (32)$$

The WIMP number density,  $n$ , is then given by the line density divided by  $4\pi r^2$ . The fits given above are optimized for small radii, as these are the most important for calculating the flux from annihilation in this halo around the Sun. Note that the densities we find here are only marginally larger than the background density of WIMPs in the galactic halo (about a factor of ten larger at the solar surface).

##### A. The halo number density dependence on the cross section and WIMP mass

The magnitude of the cross section, except for very low cross sections, is insignificant for the WIMP density around the Sun. This is due to the capture rate of galactic WIMPs in the Sun being proportional to the cross section, while the lifetime of a WIMP orbit is proportional to the inverse of the cross section. However, if the cross section is very small the finite age of the Sun can reduce the halo density since the scatter process of the captured WIMPs is for some proportion of the orbits so slow that equilibrium has simply not yet been reached. The internal relation between the spin dependent and spin independent cross section is however important, since this determines whether or not the WIMPs scatter mostly off hydrogen or mostly off heavier elements.

The WIMP density around the Sun is seen to not be all that sensitive to the WIMP mass. A heavy WIMP is more difficult for the Sun to capture but on the other hand the number of scatters needed before complete solar entrapment increases. The capture process being lengthier for heavy WIMPs makes them somewhat more sensitive to very low scatter cross sections.

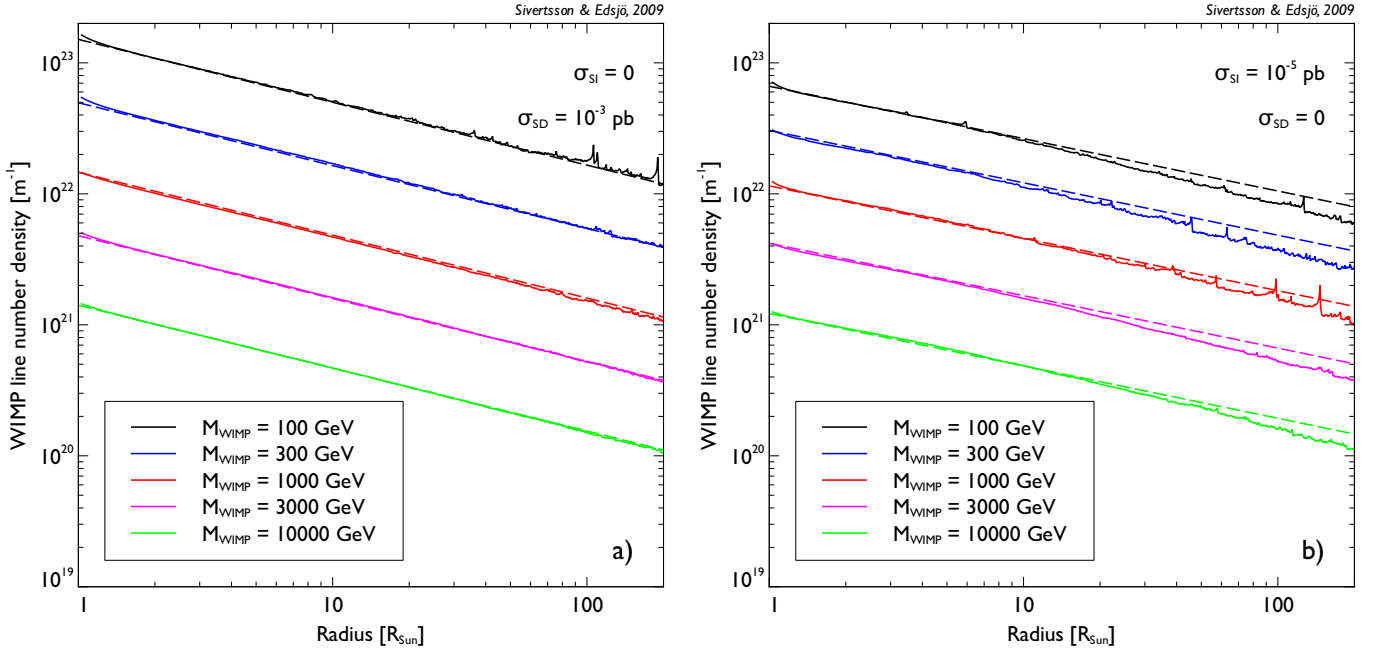


FIG. 4: a) The line number density of WIMPs around the Sun with spin dependent cross section being dominant, i.e. WIMPs do only scatter off hydrogen. In this figure  $\sigma_{SD} = 10^{-3}$  pb and  $\sigma_{SI} = 0$  pb. The dashed curves are the fits described by expression (30). b) The line number density of WIMPs around the Sun with spin-independent cross section being dominant, i.e. WIMPs scatter off all elements in the Sun. In this figure  $\sigma_{SD} = 0$  pb and  $\sigma_{SI} = 10^{-5}$  pb. The dashed curves are the fits described by expression (31).

## V. GAMMA RAY FLUXES AT EARTH

### A. Signal fluxes from WIMP annihilations in the solar halo

The number of WIMP annihilations,  $\Gamma_A$ , for a given volume is in general given by

$$\Gamma_A = \frac{1}{2} \langle \sigma v \rangle \int n^2 dV. \quad (33)$$

For simplicity, let us assume a standard annihilation cross section of  $\langle \sigma v \rangle = 3 \cdot 10^{-26} \text{ cm}^3 \text{ s}^{-1}$ , that gives about the correct relic density of WIMPs.

The flux of gamma radiation at Earth from a small source is

$$\Phi_\gamma = \Gamma_A \frac{1}{4\pi l^2} N_\gamma, \quad (34)$$

where  $l$  is the distance between the gamma ray source and the telescope at Earth. The average number of gamma rays created per WIMP annihilation,  $N_\gamma$ , requires further assumptions about the WIMP candidate investigated. We here assume that the WIMP annihilations create  $b\bar{b}$ , which give reasonably high fluxes of gamma rays. With DarkSUSY 5.0.4 [14], we have calculated that we then get about  $N_\gamma = 14.1, 45.7$  and  $94.6$  for  $M_{WIMP} = 100, 1000$  and  $10000$  GeV respectively. These  $N_\gamma$  are calculated above 1 GeV in gamma energy. We could also get monochromatic gamma rays from annihilation to  $\gamma\gamma$  and  $Z\gamma$ , but these channels produce even fewer gamma rays per annihilation and (as we will see), given the low fluxes of gamma rays we predict, it does not make any difference to our results including them or not.

Combining expressions (33) and (34) for our spherically symmetric WIMP distribution, one obtains the observed flux at Earth per solid angle

$$\frac{d\Phi_\gamma}{d\Omega} = \frac{1}{8\pi} \langle \sigma v \rangle N_\gamma \int n^2(r) dl, \quad (35)$$

which can be evaluated using  $r^2 = l^2 + R^2 - 2Rl \cos(\theta)$ , where  $R$  is the distance between the Earth and the Sun,  $\theta$  is the angle between the direction of observation and the direction towards the solar centre and  $r$  is the distance from

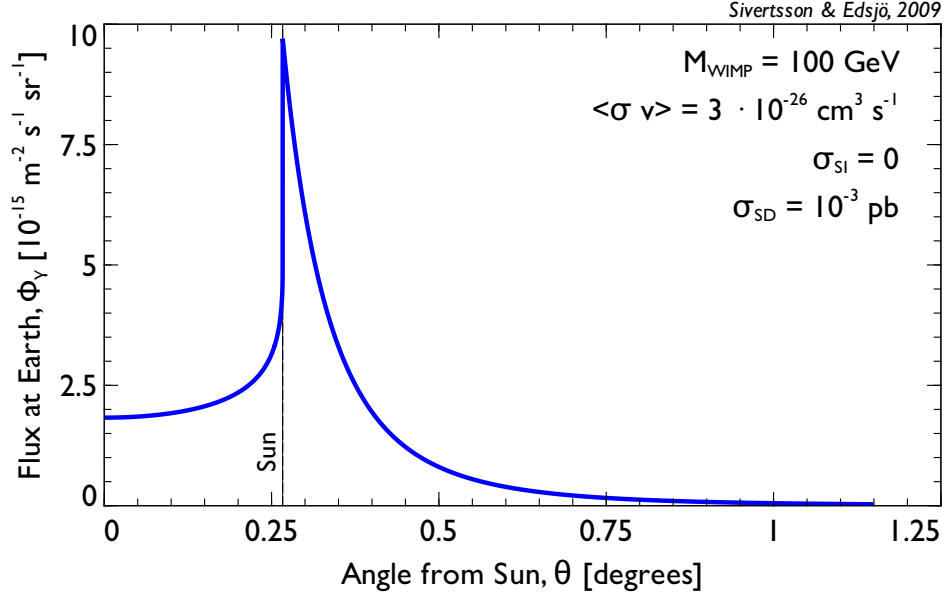


FIG. 5: The flux per solid angle from the Sun's WIMP halo as seen from Earth for  $M = 100$  GeV,  $\sigma_{SD} = 10^{-3}$  pb and  $\sigma_{SI} = 0$ . Plotted against the angle of sight  $\theta$ , looking towards the centre of the Sun corresponds to  $\theta = 0$ .

the Sun. Since gamma rays can not pass through the Sun one gets a limit in  $l$  at the Sun's surface in the integration, when the line of sight intersects the Sun, giving

$$l \leq R \cos \theta - \sqrt{R_\odot^2 - R^2 \sin^2 \theta} \quad \text{when} \quad \theta \leq \arcsin \left( \frac{R_\odot}{R} \right). \quad (36)$$

The gamma ray flux at Earth per solid angle, from expression (35), is shown for 100 GeV WIMP in figure 5. When looking just outside the rim of the Sun the graph peaks since the distance probed by the telescope suddenly increases (as does the astrophysical background). The gamma ray flux decreases fast with increasing  $\theta$  since the WIMP overdensity falls off fast with distance. Note that we have here not included the background density of WIMPs from the galactic halo, that would actually dominate for the large distances away from the Sun.

The total flux at Earth from these WIMP annihilations integrated out to some maximum angle,  $\theta_{\max}$ , is

$$\Phi_\gamma = \frac{1}{4} \langle \sigma v \rangle N_\gamma \int_0^{\theta_{\max}} \int_0^{l_{\max}} n^2(r) \sin \theta \, dl \, d\theta. \quad (37)$$

In Table I, we show this flux for some WIMP parameter configurations (integrated over all  $\theta$ , as the end result is not very sensitive on the actual value of  $\theta_{\max}$ ). One should also note that the WIMP annihilation rate in the solar halo is much lower than the capture rate and hence has no significant impact on the WIMP density in the solar halo.

Milagro has searched for gamma rays from the Sun and with their estimated integrated effective areas  $A_{\text{eff}}^T$  for these searches [4], based on 1165 hours of observation of the Sun, we can estimate the total number of events these WIMP annihilations should have produced. In Table I we give the integrated effective areas for Milagro convoluted with the gamma ray energy spectrum as calculated with DarkSUSY for annihilation to  $b\bar{b}$ ,

$$N_\gamma AT = \int_0^{M_{WIMP}} A_{\text{eff}}^T \frac{dN_\gamma}{dE} dE.$$

The total number of events in Milagro are also given in Table I. As can be seen, the total number of events are at best in the  $10^{-14}$  range, i.e. an extremely small number of events, which of course would not have shown up in the Milagro searches at all.

Compared to Milagro, there are also other gamma ray experiments that can look for a gamma ray excess from the Sun, e.g. *Fermi* [18], HAWC [19] and ARGO-YBJ [17]. Air Čerenkov telescopes cannot look at the Sun as they can only observe when the sky is dark. *Fermi* has an effective area of slightly below 1 m<sup>2</sup>, which gives a total number of events about  $10^{-10}$  for five years observation of a 100 GeV WIMP, i.e. far below any detection limit. HAWC on the

$M_{WIMP}$ (GeV)	100	100	1 000	1 000	10 000	10 000
$\sigma_{SI}$ (pb)	0	$10^{-5}$	0	$10^{-5}$	0	$10^{-5}$
$\sigma_{SD}$ (pb)	$10^{-3}$	0	$10^{-3}$	0	$10^{-3}$	0
$N_\gamma(> 1 \text{ GeV})$	14.1	14.1	45.7	45.7	94.6	94.6
$\Phi_\gamma^{>1 \text{ GeV}} (\text{m}^{-2} \text{ s}^{-1})$	$8.4 \cdot 10^{-19}$	$1.8 \cdot 10^{-19}$	$2.5 \cdot 10^{-20}$	$1.7 \cdot 10^{-20}$	$4.9 \cdot 10^{-22}$	$4.0 \cdot 10^{-22}$
$(N_\gamma AT)_{Milagro} (\text{m}^2 \text{ s})$	0	0	$1.0 \cdot 10^7$	$1.0 \cdot 10^7$	$3.4 \cdot 10^9$	$3.4 \cdot 10^9$
$N_{Milagro}$ (events)	0	0	$5.6 \cdot 10^{-15}$	$3.8 \cdot 10^{-15}$	$1.8 \cdot 10^{-14}$	$1.5 \cdot 10^{-14}$
$(N_\gamma AT)_{HAWC} (\text{m}^2 \text{ s})$	$2.9 \cdot 10^7$	$2.9 \cdot 10^7$	$7.1 \cdot 10^{10}$	$7.1 \cdot 10^{10}$	$7.5 \cdot 10^{12}$	$7.5 \cdot 10^{12}$
$N_{HAWC}$ (events)	$1.7 \cdot 10^{-12}$	$3.7 \cdot 10^{-13}$	$3.9 \cdot 10^{-11}$	$2.6 \cdot 10^{-11}$	$4.0 \cdot 10^{-11}$	$3.3 \cdot 10^{-11}$
$(N_\gamma AT)_{ARGO-YBJ} (\text{m}^2 \text{ s})$	$4.0 \cdot 10^{11}$	$4.0 \cdot 10^{11}$	$1.5 \cdot 10^{13}$	$1.5 \cdot 10^{13}$	$4.3 \cdot 10^{14}$	$4.3 \cdot 10^{14}$
$N_{ARGO-YBJ}$ (events)	$2.4 \cdot 10^{-8}$	$5.1 \cdot 10^{-9}$	$8.2 \cdot 10^{-9}$	$5.6 \cdot 10^{-9}$	$2.3 \cdot 10^{-9}$	$1.9 \cdot 10^{-9}$

TABLE I: A set of benchmark WIMP models and their corresponding gamma ray fluxes above 1 GeV at Earth from WIMP annihilations in the solar halo. Also shown are the integrated effective areas (from [4]) convoluted with the gamma ray spectrum  $dN_\gamma/dE$  for WIMP annihilations to  $b\bar{b}$ . The total number of events expected in the Milagro search for gamma rays from the Sun is also shown. For Milagro, the number of events are given for the specific search for gamma rays from the Sun that has been carried out in [4]. For HAWC and ARGO-YBJ, 5 years of observation of the Sun has been assumed with the effective areas taken from [16] and [17]. The annihilation cross section is assumed to be  $\langle\sigma v\rangle = 3 \cdot 10^{-26} \text{ cm}^3 \text{ s}^{-1}$ .

other hand will be much larger than Milagro and *Fermi* and will have an effective area about  $100 \text{ m}^2$  at 100 GeV and about few times  $10^4 \text{ m}^2$  at higher energies [16]. We have calculated  $(N_\gamma AT)$  for HAWC and the corresponding number of events in five years livetime and the number of events are at most in the  $10^{-11}$  range, i.e. very small. Even though HAWC is much bigger than *Fermi*, it has a rather high threshold of around 30 GeV and quite low effective areas for low energies, which makes the rates rather small for typical WIMP masses. ARGO-YBJ is designed to have a low energy threshold (sub-GeV) and the effective area increases rapidly with energy. At 1 TeV, the effective area is at most  $10^6 \text{ m}^2$  [17] (assuming the optimistic 1 multiplicity channel for scaler mode operation). We have calculated  $(N_\gamma AT)$  also for ARGO-YBJ given the effective areas for this mode in [17]. These and the corresponding number of events are also given in Table I. The number of events are at most in the  $10^{-8}$  range for five years livetime. Hence, the signals are really diminutive, even with the optimistic assumptions for current and future detectors used here.

## B. Backgrounds of gamma ray fluxes from the Sun

As the Sun does not shine at such high photon energies and also shields against the diffuse gamma ray background one might naively assume that this signal has essentially no background. However, secondary cosmic ray processes produce gamma rays from around the Sun. E.g., cosmic ray protons interacting with the Sun's chromosphere [7], produce a gamma ray flux of about  $10^{-4} \text{ m}^{-2} \text{ s}^{-1}$  above 1 GeV.

Solar photons can also be up-scattered in energy by cosmic ray electrons [8, 9, 10], which produce an even larger flux of gamma rays than the proton interactions. This gamma ray flux has also been measured by *EGRET* data [20], where a flux of about  $3 \cdot 10^{-3} \text{ m}^{-2} \text{ s}^{-1}$  in the energy range 100–300 MeV has been seen. Also *Fermi* has observed this gamma flux in the energy range 100 MeV–10 GeV and the preliminary results agree well with the predicted background [21]. One should also note that this background depends on the solar cycle, and as the Sun is more quiet now, we expect a slightly larger astrophysical gamma ray background at the present *Fermi* result than the older *EGRET* measurement.

Either way, comparing these background fluxes with the expected signal fluxes in Table I, we see that the expected signal is indeed extremely well hidden in the backgrounds. The proton-induced background is expected to be quite well-defined to the solar rim, whereas the inverse-Compton up-scattered photons are expected to be more extended. In both cases, the Sun itself should appear as a shadow as it blocks the cosmic rays from the other side. The WIMP signal on the other hand, should arise also from the Sun itself as is seen in figure 5. However, even if we expect a different angular distribution and energy spectrum of the signal, it is going to be virtually impossible to disentangle the WIMP signal from the backgrounds, even for an overwhelmingly huge future gamma ray detector looking towards the Sun.

## VI. DISCUSSION

This work is under the assumption that the orbiting WIMPs are not disturbed during the capture process. In reality the solar system also has planets, whose gravitational interaction can disturb the orbiting WIMPs. This effect, as caused by Jupiter, has been discussed in e.g. [22]. A massive planet, like Jupiter, can disturb orbiting WIMPs so that they end up on orbits no longer intersecting the Sun, potentially making them very long lived. On the other hand, WIMPs on orbits stretching so far out spend almost all their time far away from the Sun and hence do not contribute so much to the density close to the Sun. Furthermore, planetary interactions are more likely to throw WIMPs out of the solar system, reducing the WIMP density. WIMPs disturbed to bound orbits not intersecting the Sun end up on orbits sensitive to planetary interactions and will, in time, be disturbed again and typically lose their future contributions to the density close to the Sun. There is, however, a possibility that some fraction of these WIMPs on non-solar-crossing orbits turn out to be more stable, rendering a possible source for higher WIMP densities in the solar system. Such a mechanism has been discussed in [23, 24], where it was argued that WIMPs which scatter in the outskirts of the Sun can be perturbed by the planets to orbits not crossing the Sun, in such a way that the new orbits become stable over very long timescales. This WIMP population would then build up over time and it was argued in [23, 24] to be a significant source of WIMPs in the solar system. These calculations were analytical, but they have not been confirmed in later numerical simulations [25]. In fact, in [25], it is argued that the life-times would be much shorter and that the density enhancement would be quite small. In principle, it would be interesting to add planetary interactions to our simulations, as these could in principle increase the density somewhat (even if not as much as originally argued in [23, 24]). That is however outside the scope of this paper, as it would be a very extensive task to do. It is also unlikely that the effects would be large enough to be interesting.

Another possibility to get higher WIMP densities is from a dark matter disk [26] that would enhance the capture rate in the Sun by up to an order of magnitude [27]. If such a disk exists, it would of course also enhance the density in the WIMP halo around the Sun. The capture rates could be enhanced by up to one order of magnitude. However, as the WIMPs in the dark matter disk would have lower velocities, they would have a shorter time scale for capture, and we do not expect them to contribute as much (per WIMP) to the halo around the Sun. Even if we optimistically assume that each captured WIMP from the dark matter disk would contribute as much as a WIMP from the galactic halo, we expect at most up to two orders of magnitude enhancements to the gamma fluxes from the Sun. Even if this is a striking enhancement, the signal would still be too small to be detectable.

From the motions of the planets it is possible to set some limits on the dark matter distribution within the solar system (see e.g. [28]). However, the constraints are not very strong and far from placing any additional constraints on the WIMP densities we have found here.

The calculated gamma ray flux at Earth from WIMP annihilations around the Sun is extremely low, as seen in table I. The calculated flux, at best, corresponds to around one gamma photon per square 10 km per century, which is hardly ever detectable.

The low calculated signal in this work is in contradiction with the earlier result published by Strausz [3]. The analysis conducted here is, however, far more detailed. In [3] it is assumed that the WIMPs move in one-dimensional orbits and that they all have some sort of average properties, such as the average energy loss in a scatter and the average scatter probability in a passage through the Sun. It is, however, very unlikely for the assumptions in [3] to, by themselves, be responsible for such a strong disagreement. The passage where most of the disagreements appear is not explained in detail in [3], and hence, it is impossible to tell what the source is of the difference in results.

One should note also, that a calculation of the WIMP densities in the halo has also been performed by Fleysher [6]. Fleysher finds even larger densities than Strausz, but that calculation cannot be correct. E.g., the solar halo WIMP densities in the calculation by Fleysher are proportional to the scattering cross sections, which is unreasonable, as the scattering cross sections that enter in the probability of the first scatter and the lifetime of the WIMP orbits cancel (see section IV A for a more thorough discussion about this).

The conclusion of the work presented here, on the other hand, agrees with the conclusion argued by Hooper [5]. That work is also not very detailed but more recent than Strausz' paper. Also Peter [22] has performed simulations of WIMPs in the solar system, from which the WIMP density can be extracted. As discussed in [29] those results are very similar to the results found here. Another test of the validity of our results is performed in Appendix A.

Finally, we can note that we set out this work with the hope of proving Strausz' optimistic calculations to be correct, but unfortunately, our detailed calculations instead show that the fluxes are indeed far too small to be detectable. On top of that, there are astrophysical backgrounds in which the signal is very well hidden. To reach this conclusion we have made optimistic assumptions about the WIMP dark matter candidate. However, we have assumed that the WIMPs are thermally produced in the early Universe, i.e. has an annihilation cross section of the order of  $3 \cdot 10^{-26} \text{ cm}^3 \text{ s}^{-1}$ . Of course, non-thermal productions or other enhancements (like a Sommerfeld enhancement at low annihilation velocities) would also be possible, but given the large enhancements needed to get an observable flux of gamma rays from WIMP annihilations around the Sun, there are far better ways to search for those WIMPs in those cases, like

gamma rays from dwarf galaxies, annihilations in the galactic halo, or effects on the cosmic microwave background radiation [30].

### APPENDIX A: ARE THE RESULTS REASONABLE?

The calculated signal is truly very weak. This appendix is a further check if the results are reasonable by also estimating the density using simpler arguments. Using what we have learned about the capture process and the shape of the WIMP density profile one can, assuming that these qualitatively observations are valid, quite easily make an upper estimate of the magnitude of the WIMP density. This section studies the WIMP configuration  $M = 100$  GeV,  $\sigma_{SD} = 10^{-3}$  pb and  $\sigma_{SI} = 0$ .

The total capture rate of WIMPs by the Sun has been calculated also in previous work, with which we can compare [14]. For the WIMP configuration chosen the WIMP capture rate is then  $\Gamma_c = 2.4 \cdot 10^{23} \text{ s}^{-1}$ . Using this result, an upper estimate of the WIMP population available to build up the WIMP halo can be found by estimating an upper limit of the typical time scale for the WIMP capture process.

From the Monte Carlo simulations one finds it to be extremely unlikely for a WIMP of this kind to need more than 50 scatters for complete solar entrapment, which is easily verified to be reasonable by looking at the kinematics of the scatters. We will here assume our hypothetical WIMP to lose the same amount of energy in each of its 50 scatters, giving an upper estimate of the orbit time since it increases the proportion of large orbits.

The next assumption is that our WIMP has zero total energy before its first scatter. By this assumption the largest bound orbits are not taken into account, however, these orbits do not contribute much to the WIMP density close to the Sun, since a particle in this kind of orbit spends most of its time in the outer regions of the orbit and moves at maximum speed in the inner part.

For our WIMP to be hidden completely inside the Sun its reduced energy needs to be less than approx.  $-10^{11} \text{ m}^2 \text{ s}^{-2}$ , depending on orbit. This should here happen at scatter number 50; the WIMP's reduced energy after scatter number  $k$  is then  $\mathcal{E}(k) = -2 \cdot 10^9 k \text{ m}^2 \text{ s}^{-2}$ . The WIMP's energy after its first scatter then gives an orbit stretching out to  $r_{\text{max}} = 95R_\odot$ , which is more exact than the estimate above since the orbit needs a comparatively very low angular momentum to still cross the Sun, and  $r_{\text{max}}$  can then be determined quite well.

From these assumptions one gets an upper estimate of the total time the scattering process takes a WIMP

$$T_{\text{tot}} = \frac{1}{P} \frac{\pi G M_\odot}{\sqrt{2}} \sum_{k=1}^{50} \frac{1}{(-\mathcal{E}(k))^{3/2}} = \frac{1}{P} \frac{\pi G M_\odot}{4 \cdot 10^{27/2}} \sum_{k=1}^{50} \frac{1}{k^{3/2}} = \frac{7.7 \cdot 10^6}{P} \text{ s}, \quad (\text{A1})$$

where  $P$  is a lower estimate of the average scatter probability per lap for a WIMP in a bound orbit. The time required for a lap in a given orbit is given by expression (19). It might be worth noting that this total time for the capture process also includes the time spent in the orbital parts inside the Sun.

The total number of WIMPs orbiting the Sun at any given moment is then  $N = \Gamma_c T_{\text{tot}}$  and as discussed above they maximally stretch out to  $95R_\odot$ . Assuming that the shape of the WIMP density curve in Figure 4a is correct, the WIMP line density is proportional to  $r^{-0.48}$ . This gives the WIMP number density

$$n = \frac{0.52N}{4\pi(95^{0.52} - 1)R_\odot^{0.52}} r^{-2.48} = \frac{2.0 \cdot 10^{23}}{P} r^{-2.48} \text{ m}^{-3} \quad (\text{A2})$$

and hence, the gamma ray flux at Earth, cf. (37)

$$\Phi_\gamma = \frac{7.7 \cdot 10^{-25}}{P^2} \text{ m}^{-2} \text{ s}^{-1}. \quad (\text{A3})$$

What is left to estimate is the average scatter probability per lap. In the Monte Carlo simulations it was found for our WIMP scenario that the vast majority of the orbits has a scatter probability between  $10^{-3}$  and  $10^{-4}$  per lap, orbits with scatter probabilities of less than  $10^{-6}$  are found to be very rare. In this approximation we set  $P = 10^{-4}$ . This corresponds to the scatter probability for a WIMP that passes through the Sun on a straight line with minimum distance to the solar centre of 40% of the solar radius, which makes a reasonable lower estimate since most orbits come closer than that to the solar centre. It is easily verified that this probability is reasonable for the column density in the Sun.

For this WIMP configuration the upper estimated flux of gamma rays more energetic than 1 GeV is at Earth then finally

$$\Phi_\gamma = 8 \cdot 10^{-17} \text{ m}^{-2} \text{ s}^{-1}, \quad (\text{A4})$$

which is as expected a few orders of magnitude higher than the calculated flux from the Monte Carlo simulations of  $8.4 \cdot 10^{-19} \text{ m}^{-2}\text{s}^{-1}$ , cf. table I. Also the estimative upper limit on the gamma flux is too low to be detectable. This estimative reasoning is valid as long as the most stable, and improbable, orbits do not dominate the WIMP density.

### ACKNOWLEDGMENTS

We thank the Swedish Research Council (VR) for support. We also thank Tommy Ohlsson for pushing us to publish this paper.

- 
- [1] L. Bergstrom, Rept. Prog. Phys. **63**, 793 (2000), hep-ph/0002126.
  - [2] L. Bergstrom (2009), 0903.4849.
  - [3] S. C. Strausz, Phys. Rev. **D59**, 023504 (1999).
  - [4] R. W. Atkins et al., Phys. Rev. **D70**, 083516 (2004).
  - [5] D. W. Hooper (2001), hep-ph/0103277.
  - [6] L. Fleysher, PhD Thesis (2003), astro-ph/0305056.
  - [7] D. Seckel, T. Stanev, and T. K. Gaisser, Astrophys. J. **382**, 652 (1991).
  - [8] E. Orlando and A. Strong, Astrophys. Space Sci. **309**, 359 (2007), astro-ph/0607563.
  - [9] I. V. Moskalenko, T. A. Porter, and S. W. Digel, Astrophys. J. **652**, L65 (2006), astro-ph/0607521.
  - [10] I. V. Moskalenko, T. A. Porter, and S. W. Digel, Erratum ApJ **664**, L143 (2007).
  - [11] A. Gould, Astrophys. J. **321**, 571 (1987).
  - [12] J. N. Bahcall, A. M. Serenelli, and S. Basu, Astrophys. J. **621**, L85 (2005), astro-ph/0412440.
  - [13] N. Grevesse and A. J. Sauval, Space Science Reviews **85**, 161 (1998).
  - [14] P. Gondolo, J. Edsjö, P. Ullio, L. Bergström, M. Schelke, and E. A. Baltz, JCAP **0407**, 008 (2004), astro-ph/0406204.
  - [15] G. Eder, *Nuclear Forces: Introduction to Theoretical Nuclear Physics* (Cambridge: M.I.T. Press, 1968).
  - [16] B. Dingus (HAWC collaboration) (2009), talk at TeVPA 2009 conference.
  - [17] G. A. e. al. (ARGO-YBJ), Astropart. Phys. **30**, 85 (2008), 0807.2139.
  - [18] W. B. Atwood et al. (LAT), Astrophys. J. **697**, 1071 (2009), 0902.1089.
  - [19] G. Sinnis, A. Smith, and J. E. McEnery (2004), astro-ph/0403096.
  - [20] E. Orlando and A. W. Strong, A&A **480**, 847 (2008), 0801.2178.
  - [21] M. Brigida (Fermi LAT collaboration) (2009), talk at RICAP 2009 conference.
  - [22] A. H. G. Peter, Phys. Rev. **D79**, 103532 (2009), 0902.1347.
  - [23] T. Damour and L. M. Krauss, Phys. Rev. Lett. **81**, 5726 (1998), astro-ph/9806165.
  - [24] T. Damour and L. M. Krauss, Phys. Rev. **D59**, 063509 (1999), astro-ph/9807099.
  - [25] A. H. G. Peter, Phys. Rev. **D79**, 103531 (2009), 0902.1344.
  - [26] J. I. Read, L. Mayer, A. M. Brooks, F. Governato, and G. Lake (2009), 0902.0009.
  - [27] T. Bruch, A. H. G. Peter, J. Read, L. Baudis, and G. Lake, Phys. Lett. **B674**, 250 (2009), 0902.4001.
  - [28] J. M. Frere, F.-S. Ling, and G. Vertongen, Phys. Rev. **D77**, 083005 (2008), astro-ph/0701542.
  - [29] A. H. G. Peter (2009), 0905.2456.
  - [30] S. Galli, F. Iocco, G. Bertone, and A. Melchiorri, Phys. Rev. **D80**, 023505 (2009), 0905.0003.